

# Ultrafast enzyme immobilization over large-pore nanoscale mesoporous silica particles†

Junming Sun,<sup>a</sup> He Zhang,<sup>a</sup> Ruijun Tian,<sup>b</sup> Ding Ma,<sup>\*a</sup> Xinhe Bao,<sup>\*a</sup> Dang Sheng Su<sup>c</sup> and Hanfa Zou<sup>b</sup>

Received (in Cambridge, UK) 29th November 2005, Accepted 24th January 2006

First published as an Advance Article on the web 16th February 2006

DOI: 10.1039/b516930e

By finely tuning the TEOS/P123 molar ratio of the octane/water/P123/TEOS quadruple emulsion system and by controlling the synthesis conditions, an ultrafine emulsion system was isolated, under the confinement of which, nanoscale silica particles with ordered large mesopores ( $\sim 13$  nm) have been successfully constructed; the obtained mesoporous silica particles have an unusual ultrafast enzyme adsorption speed and the amount of enzyme that can be immobilized is larger than that of conventional mesoporous silica, which has potential applications in the fast separation of biomolecules.

Since the discovery of ordered mesoporous silicas (MPSs),<sup>1</sup> great efforts have been made on the morphological/textural control of such ordered mesoporous materials. Among these, the construction of nanoscale MPS has long been one of the most attractive targets for various groups aiming to improve the efficiency of mesopore usage and rapid mass transfer, and of great importance for applications in catalysis, adsorption, separation as well as inclusion chemistry.<sup>2</sup> To date, methodologies reported for nanoscale particles with ordered mesoporous structures involve a quenching procedure,<sup>3</sup> dilution of the reaction solutions,<sup>4</sup> spray drying,<sup>5</sup> as well as a secondary surfactant-mediated process<sup>6,7</sup> etc. Although nanoscale MPS particles are synthesized by some of the developed routes, the mesostructure domain, pore size and the degree of ordering are often limited. For instance, nanosized silica particles with ordered larger mesopores ( $>7$  nm) are rarely reported. However, in some cases, such as catalysis or biomolecule immobilization, a larger pore size is vital. Therefore, it is critical to find a facile route to synthesize nanoscale silica particles with ordered large mesopores. Based on the knowledge of our previous studies,<sup>8,9</sup> herein we present for the first time a novel emulsion confinement route for the design and synthesis of nanoscale silica particles (100–200 nm in length and 50–80 nm in width) with ordered large mesopores ( $\sim 13$  nm). The obtained nanoscale particles showed an ultrafast adsorption speed and a higher capacity in the immobilization of enzymes compared to conventional SBA-15. The adsorption equilibrium was reached within 10 min, which is essential for the fast separation of biomolecules.

<sup>a</sup>State Key Laboratory of Catalysis, Dalian Institute of Chemical Physics, The Chinese Academy of Sciences, Dalian 116023, P. R. China. E-mail: xhbao@dicp.ac.cn; dma@dicp.ac.cn

<sup>b</sup>National Chromatographic R&A Center, Dalian Institute of Chemical Physics, The Chinese Academy of Sciences, Dalian 116023, P. R. China

<sup>c</sup>Department of Inorganic Chemistry, Fritz-Haber Institute of the Max Planck Society, Berlin D-14195, Germany

† Electronic supplementary information (ESI) available: Further experimental details and additional data. See DOI: 10.1039/b516930e

Fig. 1a shows a typical HRSEM (High-Resolution Scanning Electron Microscope) image of the MPS particles prepared at 298 K (TEOS/P123 = 48, more SEM and TEM (Transition Electron Microscope) images can be found in the additional information, Figure S1†). The obtained particles are relatively uniform, being of *ca.* 50–80 nm width and 100–200 nm length. Significantly, ordered mesoporous structures with only 3–6 (100) planes across their width could easily be discerned by HRSEM, agreeing well with the TEM image (Fig. 1b). At the same time, the pore diameter judged from HRSEM and TEM is about 13 nm. To our best knowledge, at this pore size ( $>10$  nm), these are the smallest ordered MPS particles that have been synthesized.

The Small Angle X-ray Diffraction (SAXD) pattern of the sample is shown in Fig. 2a. An intensive and broad (100) diffraction peak at  $2\theta = 0.7^\circ$  ( $d = 12.6$  nm) with a hump shoulder at a higher  $2\theta$  value was resolved. A possible explanation is that the arrangement of the silica nanotubes in the ultrafine particles is

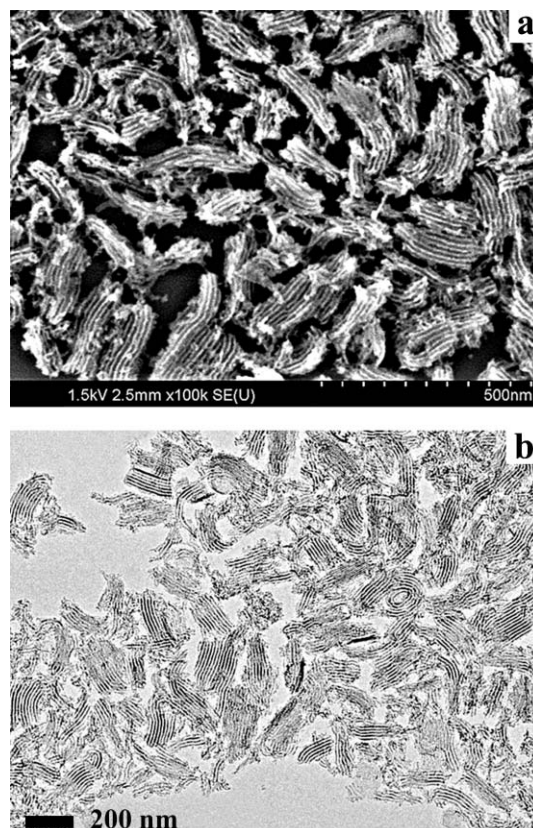


**Fig. 1** (a) HRSEM and (b) TEM images of the sample prepared with the TEOS/P123 ratio of 48 at 298 K.

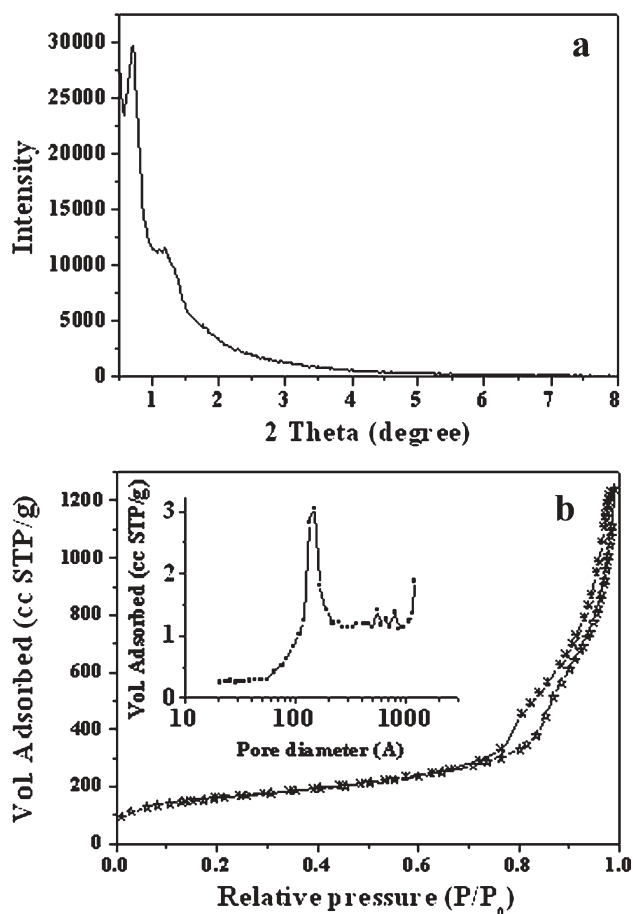


Fig. 2 (a) Small Angle X-ray Diffraction pattern and (b)  $N_2$  adsorption-desorption isotherms of the small MPS particles obtained with the TEOS/P123 = 48 at 298 K. Inset in Fig. 2b is the BJH pore diameter distribution calculated from the adsorption branch.

close to the minimum requirement for hexagonal structures, which leads to the broadening of the diffraction peaks. Fig. 2b shows the  $N_2$  adsorption-desorption isotherms of the nanoscale silica particles. It is a type IV isotherm and shows a H1 hysteresis loop at a relative pressure of about 0.85, which can be attributed to  $N_2$  capillary condensation in the MPS nanotubes. Furthermore, another intensive  $N_2$  adsorption occurred at a higher relative pressure (more than 0.9). This could be attributed to the  $N_2$  adsorption in the inter-particle spaces between the primary nanoscale mesoporous silica particles,<sup>7,10</sup> which is consistent with the SEM observation. The BET surface area of the sample is *ca.*  $565 \text{ m}^2 \text{ g}^{-1}$  and the BJH (Barrett-Joyner-Halenda) cumulative adsorption pore volume is  $1.70 \text{ cm}^3 \text{ g}^{-1}$ . The pore size distribution (calculated from the adsorption branch of the isotherms) diagram shows a tip at 13.4 nm (inset in Fig. 2b), which agrees well with the size of the mesopores detected by TEM (considering the limitations of both methods). Moreover, a series of larger pores, resulting from the inter-particle spaces, are also observed. The construction of the nanoscale MPS particles is believed to result from the confinement of an undulating, swollen inverse hexagonal phase ( $H_2$ ) in the synthesis process, details of which can be found in the supporting materials.†

Lysozyme is a model protein molecule for studying the bioimmobilization ability of MPSs.<sup>11-13</sup> It has been reported that

some chemically insignificant morphologies of MPSs (*e.g.*, traditional rope-like SBA-15) would have a great influence on the performance of enzyme immobilization. For example, rod-like SBA-15, with straight, open channels, shows a significant improvement in the immobilization of lysozyme compared to traditional SBA-15,<sup>13</sup> indicating that mesoporous materials with highly accessible porous channels are very important in their applications. In the current study,§ the obtained large-pore nanoscale MPS particles were used to immobilize lysozyme. Much to our surprise, it showed improved immobilization capacity, and most importantly, an unusual ultrafast adsorption speed over conventional SBA-15 and those others reported previously.<sup>13</sup> As indicated in Fig. 3, when the enzyme/silica ratio was 0.5, over 95% of the lysozyme was immobilized into the large-pore nanoscale silica particles within 10 min, while with conventional SBA-15, it took more than 20 h. This bioimmobilization speed is even faster than the rod-like SBA-15 reported previously,<sup>13</sup> where more than 10 h were needed to reach an adsorption equilibrium when the same conditions were used (same enzyme/silica ratio). Furthermore,  $N_2$  sorption isotherms show that the surface areas and pore diameters of the nanoscale SBA-15 with adsorbed lysozyme decreased from  $565 \text{ m}^2 \text{ g}^{-1}$  and 13.4 nm to  $235 \text{ m}^2 \text{ g}^{-1}$  and 10 nm, suggesting that most of the lysozyme molecules have been immobilized within the mesopore channels of the nanoscale SBA-15, which is consistent with the literature.<sup>12</sup> We believe that the larger pore diameter along with the smaller particle size makes the diffusion and adsorption of biomolecules easier, and most importantly, the detrimental multi-layer adsorption, which happens at a certain level of in-pore biomolecule concentration (thus blocking the immobilization of more biomolecules), will be suppressed. All these factors contribute to the observed superior enzyme immobilization behavior of the large-pore nanoscale MPS.

In summary, our results indicate that by tuning the TEOS/P123 molar ratio in the octane/water/P123/TEOS quadruple emulsion system, it is possible to construct large-pore nanoscale MPSs. The obtained nanoscale mesoporous materials show an ultrafast

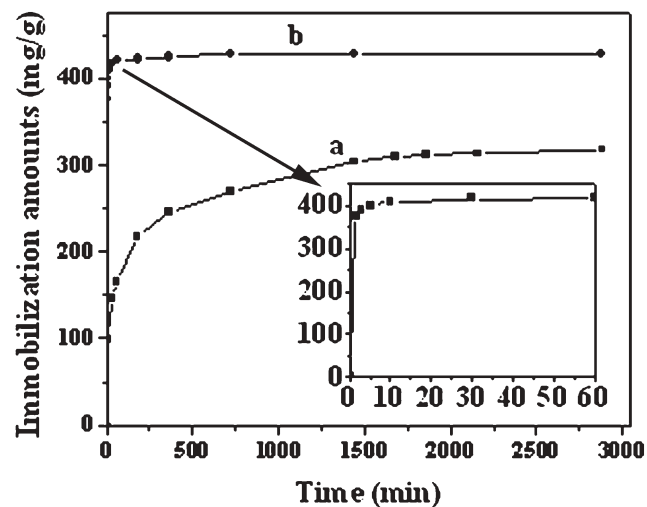


Fig. 3 Adsorption amounts of lysozymes as a function of time on different MPSs (enzyme/silica (wt/wt) = 0.5). (a) Conventional SBA-15. (b) Nanoscale MPS particles. Inset: lysozyme adsorption curve in the initial 60 min.

adsorption ability in the immobilization of enzymes, which have potential applications in the fast separation of biomolecules.¶||

We are grateful for the support of National Natural Science Foundation of China (no. 90206036) and the Ministry of Science and Technology of China (G1999022406). We thank Dr. Shuguang Li for his help with enzyme activity measurements.

## Notes and references

‡ A typical synthesis was performed as follows: 2.4 g of  $\text{EO}_{20}\text{PO}_{70}\text{EO}_{20}$  (P123) was dissolved in a 84 mL HCl solution (1.30 M) and stirred at 298 K until the solution became clear, followed by the addition of 0.027 g of  $\text{NH}_4\text{F}$ . After stirring at the same temperature for 10 min, different amounts of an octane and TEOS pre-mixture was then added under moderate stirring at the given initial reaction temperature (final P123 : HCl :  $\text{NH}_4\text{F}$  :  $\text{H}_2\text{O}$  : octane : TEOS molar ratios = 1 : 261 : 1.8 : 11278 : 235 :  $x$ ,  $x = 48$ –60). The above mixture was stirred at the given reaction temperature for 20 h and then transferred into an autoclave for further reaction at 373 K for 48 h. The products were collected by filtration, dried in air and calcined at 813 K for 5 h to remove the templates.

§ In a typical adsorption experiment, lysozymes were dissolved in sodium phosphate buffer (20 mM) at pH 7.0 to make a stock solution ( $1.0 \text{ mg mL}^{-1}$ ). Kinetic experiments to determine the amount of lysozyme adsorbed as a function of contact time were conducted by mixing 20 mL of  $1.0 \text{ mg mL}^{-1}$  protein solution with 40 mg of MPS with a gentle stirring at pH 7.0 and 25 °C in a vessel sealed to prevent evaporation (initial 0.5 (wt/wt) enzyme/silica ratio). At a given time, 1 mL of emulsion solution was extracted and then centrifugated at 15000 g for 3 min, followed by the extraction of the upper clear solution for analysis. Adsorbed amounts were measured by the difference of the concentration of the enzyme before and after UV absorption at 280 nm.

¶ SEM was undertaken on a Hitachi S4800 field-emission scanning electron microscope. The TEM image was obtained with a Philips CM 200 transmission electron microscope equipped with a CCD camera.

|| SAXD patterns were collected on a Rigaku D/MAX 2400 diffractometer equipped with a  $\text{Cu-K}_\alpha$  X-ray source operating at 40 kV and 50 mA. The  $\text{N}_2$  adsorption-desorption isotherms were recorded on an ASAP 2000 instrument.

- 1 C. T. Kresge, M. E. Leonowicz, W. J. Roth, J. C. Vartuli and J. S. Beck, *Nature*, 1992, **359**, 710; D. Zhao, J. Feng, Q. Huo, N. Melosh, G. H. Fredrickson, B. F. Chmelka and G. D. Stucky, *Science*, 1998, **279**, 548.
- 2 A. Stein, *Adv. Mater.*, 2003, **15**, 763; X. S. Zhao, G. Q. Luo and C. Song, *Chem. Commun.*, 2001, 2306; F. S. Xiao, Y. Han, Y. Yu, X. J. Meng, M. Yang and S. Wu, *J. Am. Chem. Soc.*, 2002, **124**, 888; B. G. Trewyn, C. M. Whitman and V. S.-Y. Lin, *Nano Lett.*, 2004, **4**, 2139; Y.-S. Lin, C.-P. Tsai, H.-Y. Huang, C.-T. Kuo, Y. Hung, D.-M. Huang, Y.-C. Chen and C.-Y. Mou, *Chem. Mater.*, 2005, **17**, 4570; A. Sayari, S. Hamoudi and Y. Yang, *Chem. Mater.*, 2005, **17**, 212; F. Kleitz, S. H. Choi and R. Ryoo, *Chem. Commun.*, 2003, 2136; M. Groenewolt and M. Antonietti, *Adv. Mater.*, 2005, **17**, 1789.
- 3 C. E. Fowler, D. Khushalani, B. Lebeau and S. Mann, *Adv. Mater.*, 2001, **13**, 649.
- 4 Q. Cai, Z. Luo, W. Pang, Y. Fan, X. Chen and F. Cui, *Chem. Mater.*, 2001, **13**, 258; R. I. Nooney, D. Thirunavukkarasu, Y. Chen, R. Josephs and A. E. Ostafin, *Chem. Mater.*, 2002, **14**, 4721.
- 5 Y. Lu, H. Fan, A. Stump, T. L. Ward, T. Rieker and C. J. Brinker, *Nature*, 1999, **398**, 223; S. Areva, C. Boissière, D. Grosso, T. Asakawa, C. Sanchez and M. Lindén, *Chem. Commun.*, 2004, 1630.
- 6 W. Zhao and Q. Li, *Chem. Mater.*, 2003, **15**, 4160; Y. Han and J. Y. Ying, *Angew. Chem., Int. Ed.*, 2005, **44**, 288.
- 7 K. Suzuki, K. Ikari and H. Imai, *J. Am. Chem. Soc.*, 2004, **126**, 462.
- 8 H. Zhang, J. M. Sun, D. Ma, X. H. Bao, A. Klein-Hoffmann, G. Weinberg, D. S. Su and R. Schlögl, *J. Am. Chem. Soc.*, 2004, **126**, 7440.
- 9 J. M. Sun, H. Zhang, D. Ma, Y. Chen, X. H. Bao, A. Klein-Hoffmann, N. Pfänder and D. S. Su, *Chem. Commun.*, 2005, **42**, 5343.
- 10 T. R. Pauly, Y. Liu, T. J. Pinnavaia, S. J. L. Billinge and T. P. Rieker, *J. Am. Chem. Soc.*, 1999, **121**, 8835.
- 11 J. F. Diaz and K. J. Balkus, *J. Mol. Catal. B: Enzym.*, 1996, **2**, 115; Y. J. Han, G. D. Stucky and A. Butler, *J. Am. Chem. Soc.*, 1999, **121**, 9897; J. Deere, E. Magner, J. G. Wall and B. K. Hodnett, *J. Phys. Chem. B*, 2002, **106**, 7340.
- 12 M. Hartmann, *Chem. Mater.*, 2005, **17**, 4577; Y. J. Wang and F. Caruso, *Chem. Mater.*, 2005, **17**, 953.
- 13 J. Fan, J. Lei, L. Wang, C. Z. Yu, B. Tu and D. Zhao, *Chem. Commun.*, 2003, 2140.